RSC Advances

PAPER

View Article Online
View Journal | View Issue

Cite this: *RSC Adv.*, 2020, **10**, 42204

Semi-empirical and *ab initio* calculations for crystals under pressure at fixed temperatures: the case of guanidinium perchlorate

Dmitry V. Korabel'nikov * and Yuriy N. Zhuravlev

Received 8th October 2020
Accepted 13th November 2020

DOI: 10.1039/d0ra08588j

rsc.li/rsc-advances

A simple semi-empirical approach is proposed to calculate structure and properties of crystals under pressure at fixed temperatures. The computed semi-empirical pressure dependencies for guanidinium perchlorate are in good agreement with available experimental data. *Ab initio* results within quasi-harmonic approximation for guanidinium perchlorate are also presented.

1. Introduction

The effect of external factors, such as pressure (P) and temperature (T), on crystal structure and properties has been of great interest in recent years.[1–10] Studies of the behavior of solids under pressure are very promising as it is one of the effective methods for studying intermolecular interactions.[11]

Quantum chemical *ab initio* computations within density functional theory (DFT) allow modelling crystal structure and properties, which are in good agreement with experimental results.[12] Moreover, computer modeling is used to predict and design new materials.[13] Standard *ab initio* calculations correspond to a static lattice (ground state) and do not take into account thermal effects caused by atomic thermal vibrations. Anharmonicity in interactions and thermal expansion for crystals can be considered within so-called quasi-harmonic approximation (QHA),[14] which takes into account dependence of harmonic phonon frequencies ω on the volume V. Dispersion-corrected quasi-harmonic *ab initio* computations perform well in describing thermal properties of molecular crystals.[2] The main problem within quasi-harmonic *ab initio* calculations is to determine the phonon frequency distribution $g(\omega, V)$. This is due to the fact that phonon density of states calculations are very computationally demanding tasks. The relatively simple method is quasi-harmonic Debye–Einstein (DE) approximation.[15]

The crystal structure at ambient pressure is usually known from X-ray or neutron diffraction measurements. It's well known that there is "structure–properties" relationship.[16] It's interesting to know how we can to account thermal expansion for structure of compressed crystal (thus, for its properties under pressure) based on simple standard *ab initio* calculations for static lattice and structural experimental data at ambient pressure. Therefore, it is significant to find simple semi-empirical approach to compute equation of state $P(V, T)$ and its equivalent $V(P, T)$.

Perchlorates have been widely used in explosive compositions, propellant mixtures and pyrotechnics. Guanidinium perchlorate (GP) is semi-organic nonlinear optical (NLO) and ferroelectric material.[17,18] Ferroelectric materials are widely used in many applications.[19] Besides, GP is quite attractive to be used in solid-state coolers and can provide temperature control.[18] Guanidinium perchlorate is ionic-molecular oxy-anionic crystal which has layered supramolecular structure with molecular organic guanidinium cations, $C(NH_2)_3^+$, and molecular perchlorate anions, ClO_4^-. Under ambient conditions, it has trigonal structure (space group symmetry $R3m$).[20] The experimental ambient lattice constants a and c for its hexagonal unit cell (with 3 formula units) are equal to 7.606 Å and 9.121 Å, respectively.[20] Perchlorate anions in guanidinium perchlorate contain two nonequivalent oxygen atoms O1 and O2. The knowledge of the behavior of GP and similar supramolecular structures under external pressure is important both for fundamental and applied research.[21,22] The pressure effect on the guanidinium perchlorate structure was experimentally studied using Raman spectroscopy and X-ray diffraction at room temperature.[21,22] Strong anisotropy of GP linear compressibility was shown. GP is stable up to 4.5 GPa, after that it undergoes a phase transition. The GP structural data at various fixed temperatures ($T \sim 100$–400 K) were studied in ref. 18. Thermal measurements for GP show that it undergoes a phase transition at $T \sim 450$ K.[18,23] The results of optical and nonlinear optical studies for GP were reported in ref. 17. As we know, data on pressure dependencies of structure at low temperatures (below room temperature), band gap, elastic constants and electron density topological properties were not reported for GP. In the present work we studied GP under pressure with account of thermal effects based on semi-empirical and *ab initio* calculations.

Institute of Fundamental Sciences, Kemerovo State University, Krasnaya 6, 650043, Kemerovo, Russia. E-mail: dkorabelnikov@yandex.ru

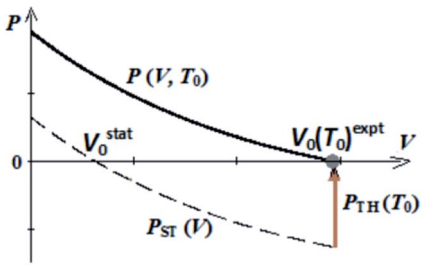

Scheme 1 Pressure–volume dependencies for static lattice (P_{ST} (V)) and for crystal at fixed temperature (P (V, T_0)) according to semi-empirical approach ($V_0 = V_0$ (T_0)^{expt}).

2. Computational details

Ab initio calculations were performed using CRYSTAL program.[24] Basis sets of atomic orbitals[25–28] and dispersion-corrected generalized-gradient PBE DFT functional[29,30] were used in our calculations. Grimme's dispersion correction[30] was used in order to include the long-range intermolecular interactions. Structural parameters for static lattice were calculated by geometry optimization (all atoms positions and cell lengths) in accordance with BFGS algorithm.[31] Energy convergence was better than at 10^{-8} a.u. Chemical bond was studied based on Bader's quantum theory of atoms in molecules (QTAIM).[32] Energies of hydrogen bonds were evaluated using potential energy density at bond critical points.[33] The TOPOND code[34] was used for QTAIM electron density topological analysis. We used quasi-harmonic DE approximation[15] to include thermal effects based on *ab initio* calculations. *Ab initio* frequencies were computed using diagonalization of the mass-weighted Hessian matrix of second energy derivatives with respect to atomic displacements.[24] Vinet universal equation of state[35] (EOS) was fitted to pressure-volume data. Three parameters determine this EOS: equilibrium volume (V_0), bulk modulus (B_0) and its pressure derivative ($\partial B_0/\partial P$).

It's known[36] that pressure can be expressed as P (V, T) = P_{ST} (V) + P_{TH} (V, T), where P_{ST} (V) = $-\partial E_{ST}$ (V)/∂V is static pressure

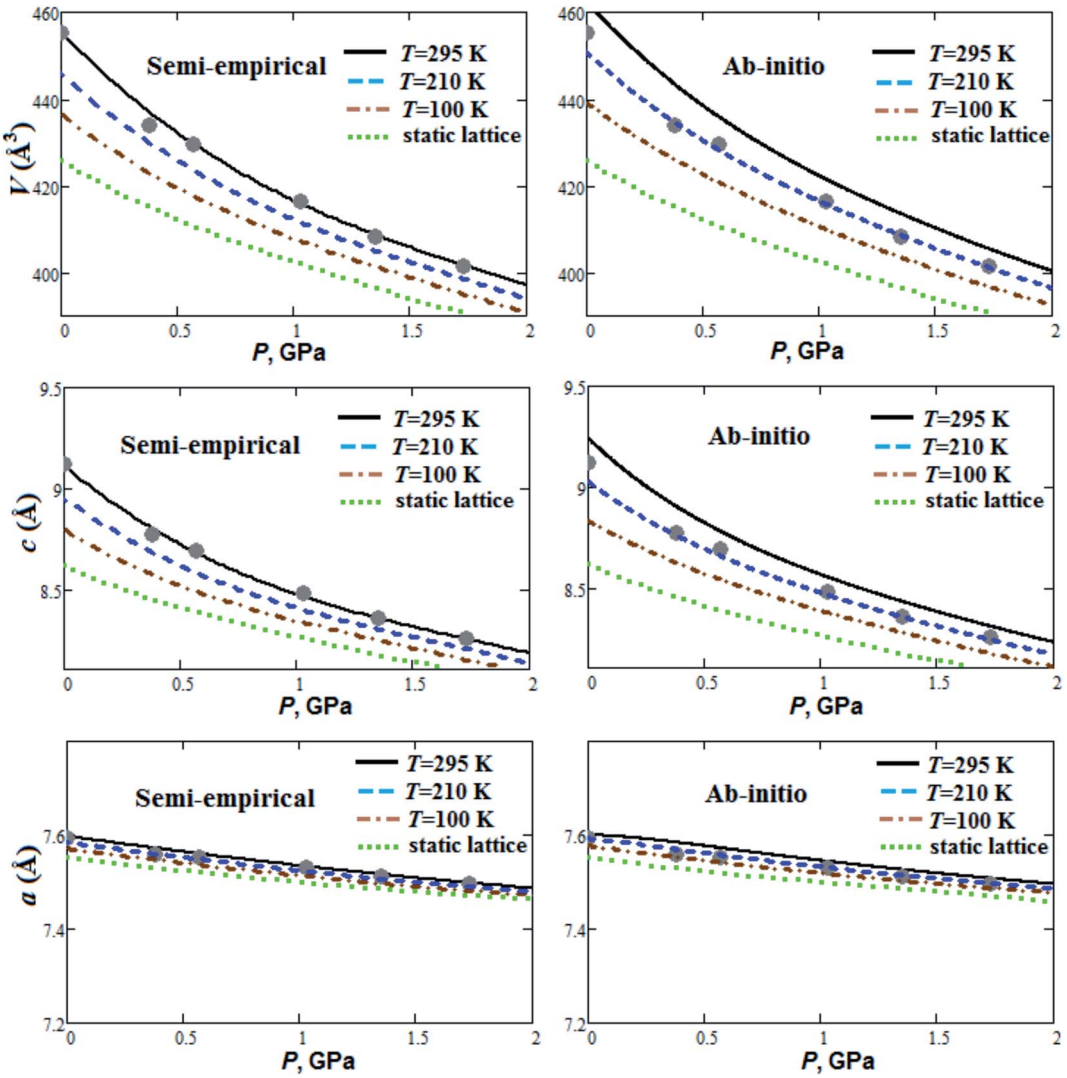

Fig. 1 Calculated semi-empirical and *ab initio* pressure dependencies of lattice parameters and volume for guanidinium perchlorate at T = 295 K (solid lines), 210 K (dashed lines), 100 K (dash-dotted lines) and at static lattice (dotted lines). Experimental points correspond to T = 295 K.[22]

($E_{ST}(V)$ is *ab initio* static energy) and $P_{TH}(V, T) = -\partial F_{vib}(V, T)/\partial V$ is thermal pressure ($F_{vib}(V, T)$ is vibrational part of the Helmholtz free energy). Within the framework of the quasi-harmonic approximation the thermal pressure $P_{TH}(V, T)$ can be expressed as $P_{TH}(V,T) = \sum_i f_i(V)(0.5 + (e^{\hbar\omega_i/kT} - 1)^{-1})$, where $f_i(V) = \hbar\omega_i\gamma_i/V$ (ω_i and γ_i are the frequency and Gruneisen's parameter of i-th vibrational mode, respectively).[14] The functions $f_i(V)$ are equal to constants $\hbar \cdot b_i$ within the frequency linear approximation ($\omega_i = a_i - b_i \cdot V$). Thermal pressure is weakly dependent on V and, therefore, $P_{TH}(V, T) \approx P_{TH}(T)$.[37] So, volume-pressure dependencies at fixed temperatures T_0 (isotherms $P(V, T_0)$) can be obtained through shift of static pressure function $P_{ST}(V)$ by $P_{TH}(T_0)$. Thermal pressure $P_{TH}(T_0)$ should correspond to equilibrium volume V_0 at fixed temperature T_0.

Ab initio thermal pressures were found based on *ab initio* calculations of frequencies ω_i within quasi-harmonic approximation. In contrast to *ab initio* method, we used experimental equilibrium volumes in semi-empirical approach to find thermal pressures P_{TH} without *ab initio* calculations of frequencies. In the present work we propose to set the equilibrium volumes V_0 for isotherms $P(V, T_0)$ as equal to experimental ones $V_0(T_0)^{expt}$ (Scheme 1). So, $P_{TH}(T_0) = -P_{ST}(V_0^{expt})$.

Thermal pressure for guanidinium perchlorate at room temperature obtained in our work within semi-empirical approach (0.68 GPa) is comparable with its *ab initio* value (0.78 GPa).

Table 1 Calculated equation of state parameters (V_0, B_0, $\partial B_0/\partial P$) for guanidinium perchlorate at different temperatures. Experimental data are given for $T = 295$ K (ref. 22)

Temperature	Method	V_0	B_0	$\partial B_0/\partial P$
$T = 295$ K	Expt.[22]	455	6.93	11.4
	Semi-empirical	455	7.35	10.0
	Ab initio	462	7.43	8.83
$T = 210$ K	Semi-empirical	446	9.14	9.51
	Ab initio	451	9.10	8.66
$T = 100$ K	Semi-empirical	437	11.1	9.06
	Ab initio	439	11.2	8.49
Static lattice	Semi-empirical	426	13.7	8.55
	Ab initio	426	13.7	8.55

3. Results and discussion

Fig. 1 presents our calculated semi-empirical and *ab initio* pressure dependencies of lattice parameters and volume for guanidinium perchlorate at $T = 295$ K (solid lines), 210 K (dashed lines), 100 K (dash-dotted lines) and at static lattice (dotted lines). Calculated equation of state parameters (V_0, B_0, $\partial B_0/\partial P$) for GP at different temperatures are presented in Table 1. Experimental data are given for $T = 295$ K.[22] It can be seen that *ab initio* method within quasi-harmonic Debye–Einstein approximation overestimated structural parameters in comparison with experimental data. It should be noted that *ab initio* equilibrium volumes (V_0) at room temperature are also

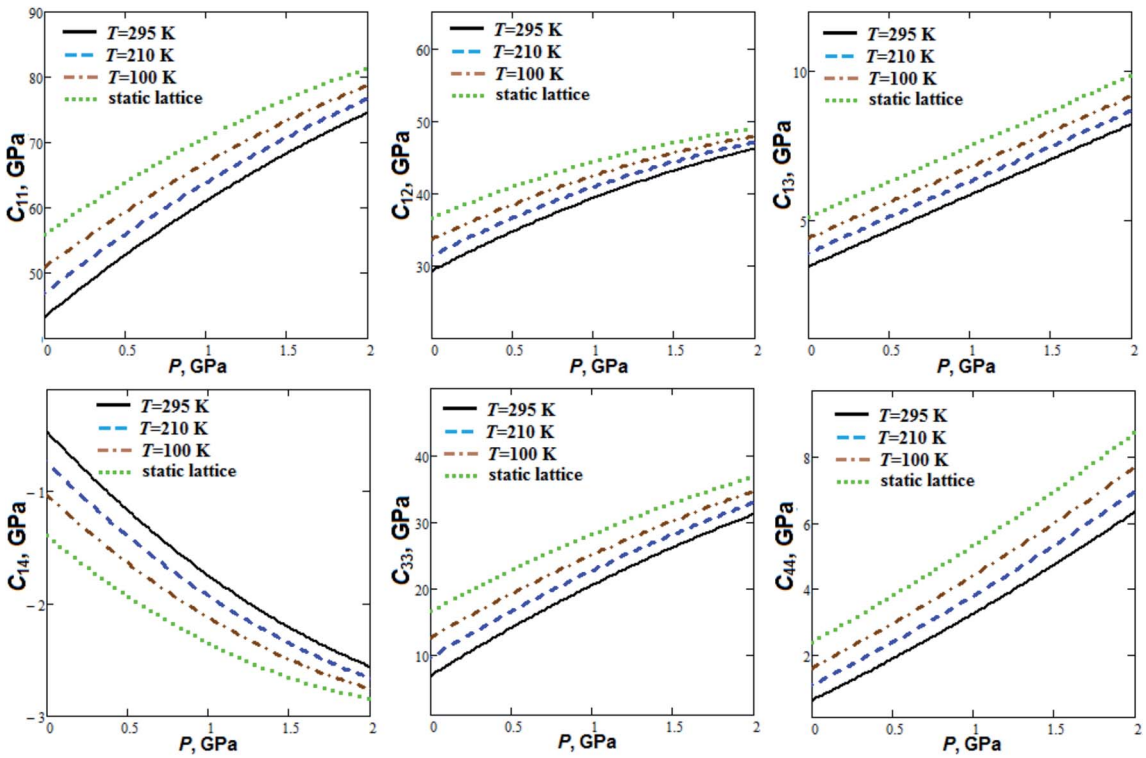

Fig. 2 Calculated independent elastic constants as semi-empirical functions of pressure for guanidinium perchlorate at $T = 295$ K (solid lines), 210 K (dashed lines), 100 K (dash-dotted lines) and at static lattice (dotted lines). $C_{11} = 43.3$, $C_{12} = 29.3$, $C_{13} = 3.4$, $C_{14} = -0.5$, $C_{33} = 6.9$, $C_{44} = 0.6$ GPa (at $T = 295$ K).

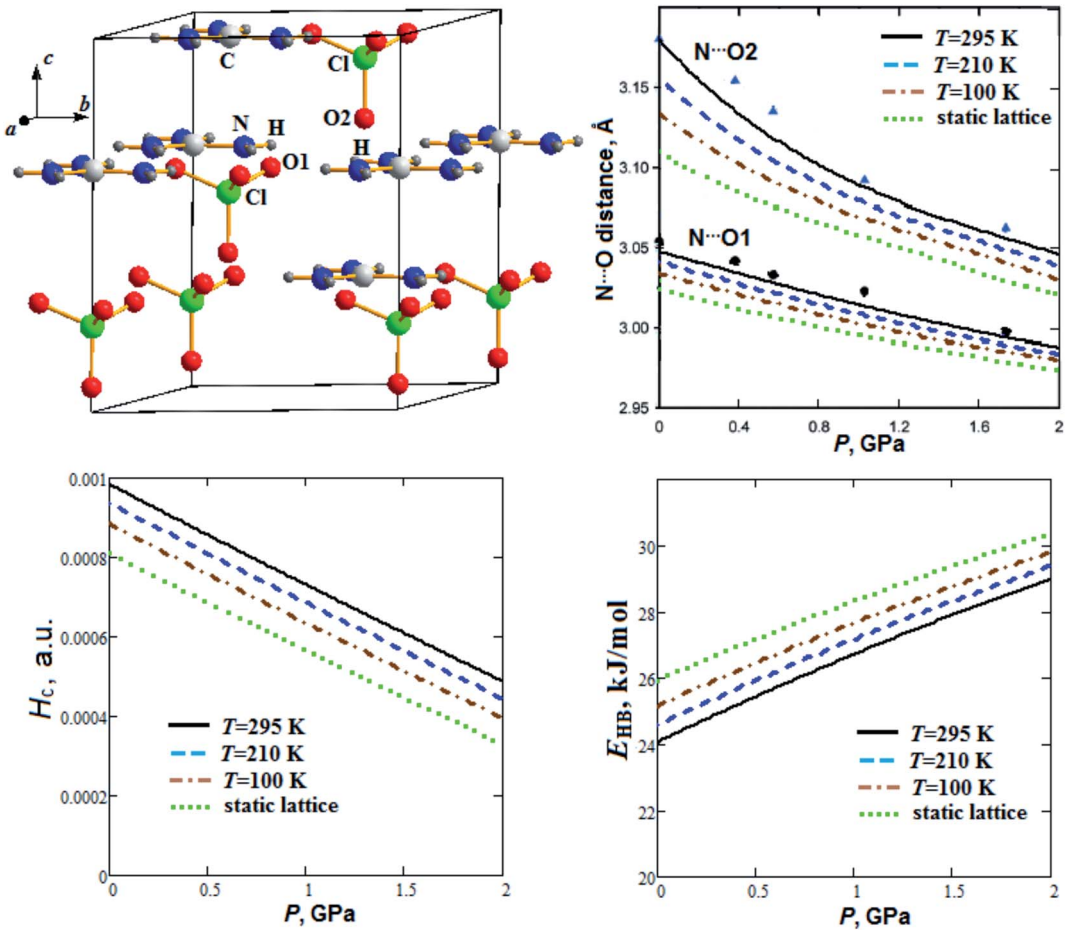

Fig. 3 Calculated semi-empirical pressure dependencies of N···O distances, energy density H_c at H···O1 critical points and hydrogen bond energy E_{HB} for guanidinium perchlorate at $T = 295$ K (solid lines), 210 K (dashed lines), 100 K (dash-dotted lines) and at static lattice (dotted lines). Experimental points and triangles correspond to $T = 295$ K.[22]

overestimated (~1%) for RDX and TATB crystals.[2] More powerful and time-consuming *ab initio* methods need to be used for stricter account of anharmonicity effects in GP, RDX and TATB. On the other hand, the results obtained, using simple semi-empirical method, agree well with experiment (Fig. 1).

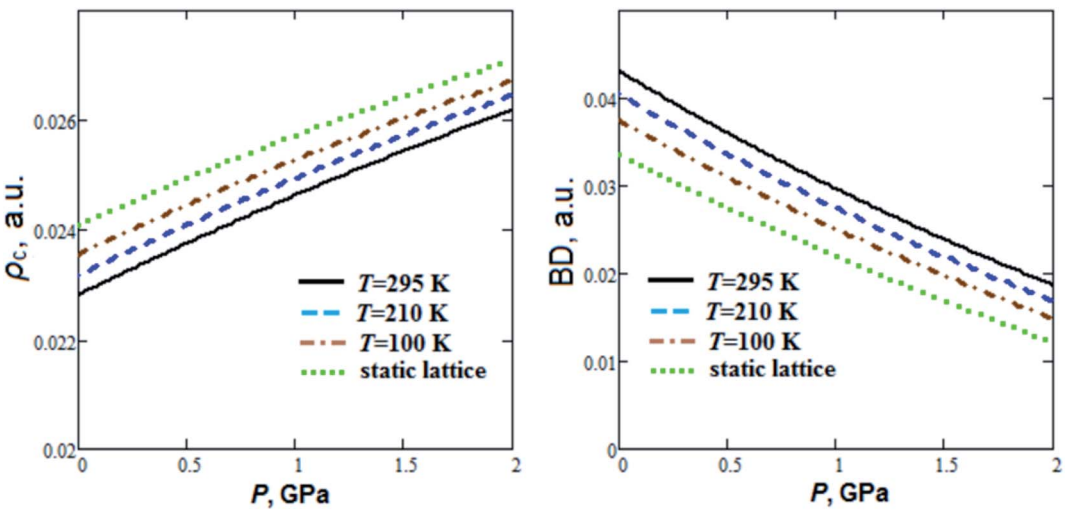

Fig. 4 Calculated semi-empirical pressure dependencies of electron density at bond critical points (ρ_c) and bond degree (BD) for hydrogen bonds in guanidinium perchlorate at $T = 295$ K (solid lines), 210 K (dashed lines), 100 K (dash-dotted lines) and at static lattice (dotted lines).

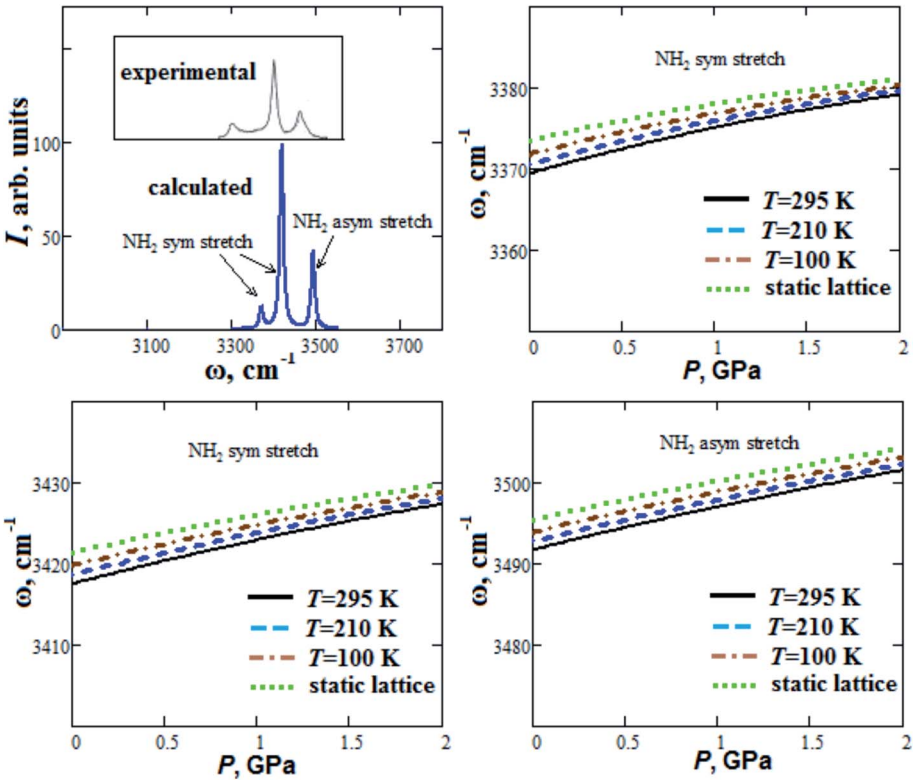

Fig. 5 Calculated Raman spectrum and semi-empirical pressure dependencies of frequencies ω of NH_2 stretch modes for guanidinium perchlorate at $T = 295$ K (solid lines), 210 K (dashed lines), 100 K (dash-dotted lines) and at static lattice (dotted lines). Experimental Raman spectrum corresponds to ambient conditions.[21]

The GP compressibility along *a*-axis is much less than along *c*-axis (Fig. 1). So, there is strong compressibility anisotropy for GP. This can occur due to layered structure of GP with strong covalent and hydrogen bonds in *ab* plane (Fig. 3). GP is highly compressible material (Fig. 1) with relatively small bulk modulus ~7 GPa at $T = 295$ K (Table 1), which is even smaller than room temperature bulk moduli for some molecular crystals reported in ref. 2. It is interesting to note that our calculated semi-empirical bulk moduli are in good agreement with *ab initio* moduli (Table 1). Fig. 1 demonstrates nonlinearity of pressure dependencies for *c* parameter and volume of GP. Such pressure behavior results in relatively high pressure derivative of B_0 (Table 1). With temperature increase from 100 K up to 295 K equilibrium volume V_0 increases by 4.1 and 5.2% within semi-empirical and *ab initio* approaches, respectively (Table 1). At the same time, this thermal volume expansion results in considerable decrease of B_0 (~33%). So, it is important to take into account thermal effects for behavior under pressure and mechanical properties of GP.

Pressure dependencies of GP elastic constants at fixed temperatures (Fig. 2) were computed according to quasi-static approach[38] and semi-empirical volume–pressure–temperature dependencies.

The elastic stability conditions[39] (the Born criteria) are fulfilled for GP. C_{11} elastic constant is considerably greater (~4 to 6 times) than C_{33}. This is due to the layered structure of GP (Fig. 3) with strong intralayer interactions (covalent and hydrogen bonds) in *ab* plane. C_{44} elastic constant has a relatively small value at room temperature (0.63 GPa). C_{11} and C_{12} elastic constants increase by 72 and 58% at room temperature whereas C_{13}, C_{14}, C_{33} and C_{44} increase by a factor of 1.4, 4.4, 3.5 and 9.1, respectively, when the pressure increases up to 2 GPa. On the other hand, elastic constants C_{11} and C_{12} at ambient pressure decrease by 15 and 13%, whereas C_{13}, C_{14}, C_{33} and C_{44} by 22, 54, 45 and 61%, respectively, when the temperature increases from $T = 100$ K up to $T = 295$ K.

Fig. 3 presents our calculated semi-empirical pressure dependencies of N···O distances, energy density at hydrogen bond critical points (H_c) and hydrogen bond energy (E_{HB}) for guanidinium perchlorate at $T = 295$ K (solid lines), 210 K (dashed lines), 100 K (dash-dotted lines) and at static lattice (dotted lines). Experimental points and triangles are given for $T = 295$ K.[22] Fig. 3 reveals that interlayer N···O2 distance decreases with pressure more significantly than intralayer N···O1 distance, similar to *c* and *a* parameters, respectively (Fig. 1). It can also be seen that GP cooling down to $T = 100$ K leads to reduction of N···O2 distance by 1.5%.

The electron density topological analysis, in the framework of the QTAIM, is a powerful chemical bond study method.[40] The condition for chemical bond formation is the presence of so-called bond critical point (BCP).[32] Electron density (ρ_c) and energy density at the bond critical point (H_c) are important characteristics. $H_c > 0$ corresponds to non-covalent closed shell interactions (electrostatic or dispersion), while at $H_c < 0$ (ρ_c is

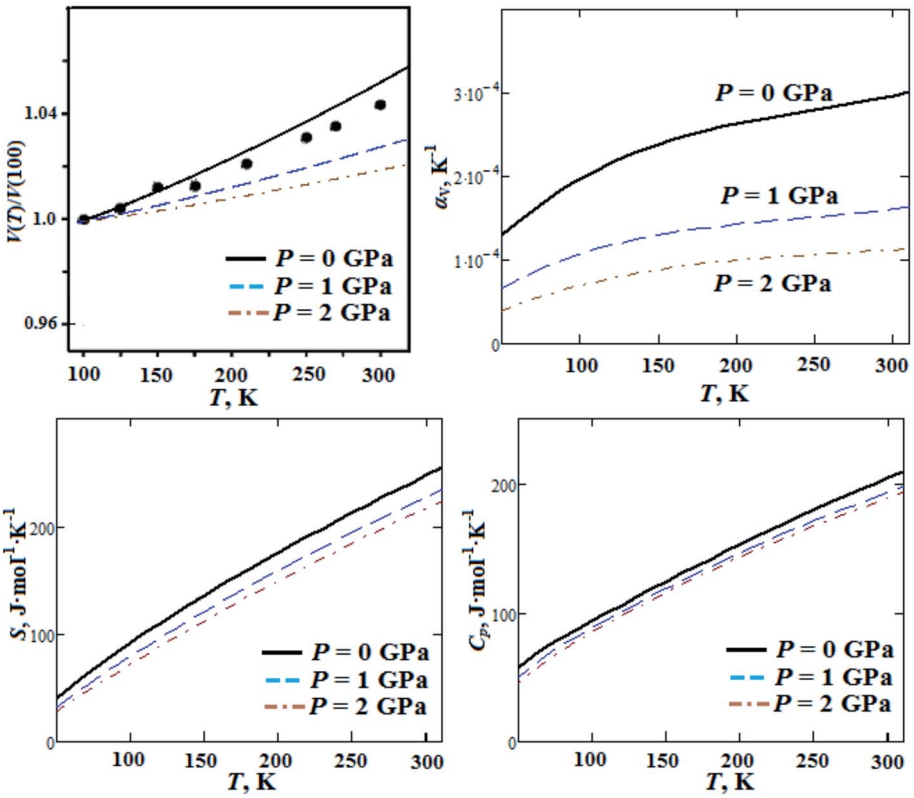

Fig. 6 Calculated temperature dependencies of relative volume, volume thermal expansion coefficient, entropy S and heat capacity C_p for guanidinium perchlorate at ambient pressure (solid lines), $P = 1$ GPa (dashed lines) and $P = 2$ GPa (dash-dotted lines). Experimental points correspond to ambient pressure.[18]

stabilizing) the bond has a covalent component (covalent or partly covalent interactions).[41] One of the superiority of Bader QTAIM approach is the possibility to reveal even weak bonding interatomic interactions and calculate their energies.[42]

As can be seen from Fig. 3, energy density H_c nearly linearly decreases with pressure increase. At the same time hydrogen bond energy ($E_{HB} \sim 24$–26 kJ mol^{-1}) increases by ~20% when the pressure increases up to 2 GPa. E_{HB} at ambient pressure decreases by 4.5% when the temperature increases from $T =$ 100 K up to $T = 295$ K. Extrapolations for pressure dependencies of energy density give negative values of H_c at pressures more than 4.2, 3.8 and 3.5 GPa for 295 K, 210 K and 100 K,

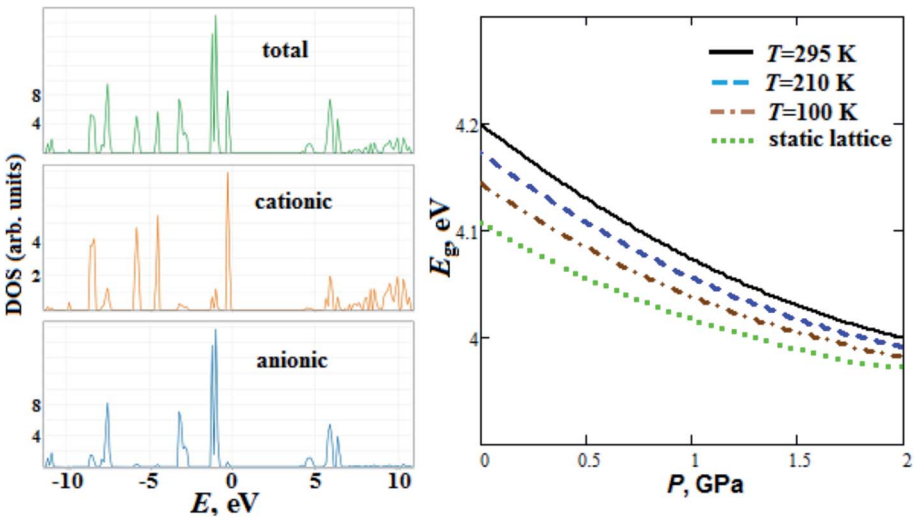

Fig. 7 Calculated anionic, cationic and total densities of states DOS (the energy of highest occupied states was set to zero), semi-empirical pressure dependencies of band gap E_g for guanidinium perchlorate at $T = 295$ K (solid lines), 210 K (dashed lines), 100 K (dash-dotted lines) and at static lattice (dotted lines).

respectively. So, the GP hydrogen bonds at pressure ~4 GPa become partially covalent in nature. Electrostatic and partially covalent nature of hydrogen bonds for other crystals and molecular complexes was studied earlier in ref. 43. It is interesting to note that GP at P ~4 GPa undergoes a phase transition.[21] The electron density at BCP ($\rho_c \sim 0.023$ a.u.) increases by ~15%, whereas bond degree parameter[44] ($BD = H_c/\rho_c$) decreases ~2 times as the pressure rises to 2 GPa (Fig. 4). On the other hand, when the temperature increases from $T = 100$ K up to $T =$ 295 K, ρ_c at ambient pressure decreases and BD increases by 3.2% and 15%, respectively.

Our calculated Raman spectrum of GP for NH_2 stretch modes in comparison with experimental spectrum[21] is given in Fig. 5. It shows three maximums at 3371, 3419 and 3493 cm^{-1}, which are in agreement with experimental ones within 2%. In general, blue or red shift can occur when hydrogen bond length decreases.[45] Our calculated frequencies of NH_2 stretch modes increase with pressure increase up to 2 GPa (blue shift ~10 cm^{-1}) in accordance with experimental data reported in ref. 21. As it was pointed out in ref. 21, this reflects the strengthening of hydrogen bonds in GP with increasing pressure. When the temperature increases from $T = 100$ K up to $T =$ 295 K, our calculated frequencies ω of NH_2 stretch modes at ambient pressure decreases by ~2 cm^{-1} (Fig. 5).

In our previous works we reported *ab initio* investigations of thermal properties for alkali metal nitrates, chlorates and perchlorates.[46] In the present work we performed *ab initio* calculations of GP thermal properties (thermal expansion, entropy and heat capacity) as functions of temperature for pressures $P = 0$, 1, 2 GPa (Fig. 6). The computed volume thermal expansion is in reasonable agreement with experimental data reported in ref. 18. The calculated volume thermal expansion coefficient is ~3 × 10^{-4} K^{-1} (at room temperature) and it decreases ~3 times when the pressure increases up to 2 GPa. The computed room temperature entropy is 241 J mol^{-1} K^{-1} and it decreases by 12.5% with pressure increase up to 2 GPa. Heat capacity almost linearly increases with temperature increase from 50 K and it has value of ~200 J mol^{-1} K^{-1} at room temperature, this is in reasonable agreement with experimental data (ref. 18). It decreases by 7.8% as the pressure grows up to 2 GPa. On the other hand, volume thermal expansion coefficient α_V, entropy S and heat capacity C_p at ambient pressure increase by a factor of 1.5, 2.7 and 2.2, respectively, when the temperature increases from $T = 100$ K up to $T = 295$ K. It should be noted that thermal expansion, entropy and heat capacity for GP are much higher (~1.5 to 2 times) than the ones for alkali metal perchlorates.[46] This can occur due to large molecular polyatomic guanidinium cations in GP.

We have also calculated GP total and partial (anionic and cationic) densities of electronic states (Fig. 7). The GP lower unoccupied states have anionic nature, whereas upper valence states for GP, in contrast to alkali metal perchlorates,[47] mainly corresponds to cationic states. Our calculated GP band gap energy E_g (4.2 eV) at room temperature is comparable with experimental one (4.9 eV) reported in ref. 17. We should note that the calculated E_g for perchlorate with organic guanidinium cation is smaller (by ~10%) than E_g for alkali metal perchlorates reported in ref. 47. The band gap of GP, in contrast to alkali metal perchlorates,[47] decreases with pressure (Fig. 7).

So, E_g at room temperature decreases by ~5 and 1.4% when the pressure increases up to 2 GPa and the temperature decreases down to $T = 100$ K, respectively.

4. Conclusions

Thus, in this work we proposed simple semi-empirical method to calculate structure and properties of crystals under pressure at fixed temperatures. Only one experimental parameter (equilibrium volume) is used in this approach for isothermal pressure dependencies. We performed semi-empirical and *ab initio* calculations for guanidinium perchlorate, which allowed us to find pressure dependencies for its structure and properties (electronic, elastic, vibrational, thermal). We showed high compressibility and importance of taking into account of thermal effects for GP pressure behavior and mechanical properties. Pressure dependencies for interlayer and intralayer N···O distances correlate with c and a parameters, respectively. Moreover, we showed that hydrogen bond energy increases when the pressure increases. We revealed that GP hydrogen bonds become partially covalent in nature near the phase transition pressure. We also established that GP volume thermal expansion coefficient significantly decreases while the pressure increases. It was found out that the band gap of GP, in contrast to alkali metal perchlorates, decreases with pressure.

Conflicts of interest

There are no conflicts to declare.

References

1 E. Zurek and W. Grochala, *Phys. Chem. Chem. Phys.*, 2015, **17**, 2917.
2 (*a*) A. Erba, J. Maul and B. Civalleri, *Chem. Commun.*, 2016, **52**, 1820–1823; (*b*) A. C. Landerville, M. W. Conroy, M. M. Budzevich, Y. Lin, C. T. White and I. I. Oleynik, *Appl. Phys. Lett.*, 2010, **97**, 251908.
3 (*a*) B. A. Zakharov and E. V. Boldyreva, *CrystEngComm*, 2019, **21**, 10; (*b*) A. Y. Fedorov, D. A. Rychkov, E. A. Losev, T. N. Drebushchak and E. V. Boldyreva, *Acta Crystallogr., Sect. C: Cryst. Struct. Commun.*, 2019, **75**, 598–608; (*c*) A. A. Sidelnikov, S. A. Chizhik, B. A. Zakharov, A. P. Chupakhin and E. V. Boldyreva, *CrystEngComm*, 2016, **18**, 7276.
4 A. D. Fortes, E. Suard and K. S. Knight, *Science*, 2011, **331**, 742.
5 (*a*) F. Colmenero, *Mater. Adv.*, 2020, **1**, 1399–1426; (*b*) F. Colmenero, J. Plasil, V. Timon and J. Cejka, *RSC Adv.*, 2020, **10**, 31947.
6 (*a*) B. M. Abraham, B. Adivaiah and G. Vaitheeswaran, *Phys. Chem. Chem. Phys.*, 2019, **21**, 884–900; (*b*) N. Yedukondalu and G. Vaitheeswaran, *J. Phys. Chem. C*, 2019, **123**, 2114–2126.

7 (*a*) C. J. McMonagle, P. Comar, G. S. Nichol, D. R. Allan, J. Gonzalez, J. A. Barreda-Argueso, F. Rodriguez, R. Valiente, G. F. Turner, E. K. Brechin and S. A. Moggach, *Chem. Sci.*, 2020, **11**, 8793–8799; (*b*) S. K. Filatov, M. G. Krzhizhanovskaya, R. S. Bubnova, A. P. Shablinskii, O. L. Belousova and V. A. Firsova, *Struct. Chem.*, 2016, **27**, 1663.

8 (*a*) S. G. Kozlova and S. P. Gabuda, *Sci. Rep.*, 2017, **7**, 11505; (*b*) A. R. Aliev, M. M. Gafurov, I. R. Akhmedov, M. G. Kakagasanov and Z. A. Aliev, *Phys. Solid State*, 2018, **60**, 1203; (*c*) A. R. Aliev, I. R. Akhmedov, M. G. Kakagasanov and Z. A. Aliev, *Phys. Solid State*, 2020, **62**, 998.

9 (*a*) D. V. Korabel'nikov and Yu. N. Zhuravlev, *Phys. Chem. Chem. Phys.*, 2016, **18**, 33126; (*b*) D. V. Korabel'nikov and Yu. N. Zhuravlev, *J. Phys. Chem. A*, 2017, **121**, 6481; (*c*) I. A. Fedorov, *Comput. Mater. Sci.*, 2017, **139**, 252–259.

10 (*a*) R. A. Evarestov and A. Kuzmin, *J. Comput. Chem.*, 2020, **41**, 1337–1344; (*b*) I. S. Lyubutin, A. G. Gavriliuk, N. D. Andryushin, M. S. Pavlovskiy, V. I. Zinenko, M. V. Lyubutina, I. A. Troyan and E. S. Smirnova, *Cryst. Growth Des.*, 2019, **19**, 6935–6944.

11 (*a*) E. V. Boldyreva, *J. Mol. Struct.*, 2004, **700**, 151; (*b*) V. V. Boldyrev, *Russ. Chem. Rev.*, 2006, **75**, 177.

12 A. D. Becke, *J. Chem. Phys.*, 2014, **140**, 18A301.

13 A. R. Oganov and C. W. Glass, *J. Phys.: Condens. Matter*, 2008, **20**, 064210.

14 S. Baroni, P. Giannozzi and E. Isaev, *Rev. Mineral. Geochem.*, 2010, **71**, 39–57.

15 A. Otero-de-la-Roza, D. Abbasi-Perez and V. Luana, *Comput. Phys. Commun.*, 2011, **182**, 2232–2248.

16 D. A. Druzhbin, T. N. Drebushchak, V. S. Min'kov and E. V. Boldyreva, *J. Struct. Chem.*, 2015, **56**, 317–323.

17 S. Sivashankar, R. Siddheswaran and P. Murugakoothan, *Mater. Chem. Phys.*, 2011, **130**, 323–326.

18 M. Szafranski, *J. Phys. Chem. B*, 2011, **115**, 8755–8762.

19 J. F. Scott, *Science*, 2007, **315**, 954–959.

20 A. E. Koziol, *Z. Kristallogr.*, 1984, **168**, 313–315.

21 (*a*) S. Li, Q. Li, K. Wang, X. Tan, M. Zhou, B. Li, B. Liu, G. Zou and B. Zou, *J. Phys. Chem. B*, 2011, **115**, 11816–11822; (*b*) K. Wang, S. Li, X. Tan, G. Xiao, B. Liu and B. Zou, *Chin. Sci. Bull.*, 2014, **59**, 5258.

22 M. Szafranski, *CrystEngComm*, 2014, **16**, 6250–6256.

23 M. R. Udupa, *Propellants, Explos., Pyrotech.*, 1983, **8**, 109.

24 (*a*) R. Dovesi, R. Orlando, B. Civalleri, C. Roetti, V. R. Saunders and C. M. Zicovich-Wilson, *Z. Kristallogr.*, 2005, **220**, 571–573; (*b*) R. Dovesi, R. Orlando, A. Erba, C. M. Zicovich-Wilson, B. Civalleri, S. Casassa, L. Maschio, M. Ferrabone, M. De La Pierre and Ph D'Arco, *Int. J. Quantum Chem.*, 2014, **114**, 1287.

25 F. Cora, *Mol. Phys.*, 2005, **103**, 2483–2496.

26 C. Gatti, V. R. Saunders and C. Roetti, *J. Chem. Phys.*, 1994, **101**, 10686.

27 R. Dovesi, E. Ermondi, E. Ferrero, C. Pisani and C. Roetti, *Phys. Rev. B: Condens. Matter Mater. Phys.*, 1984, **29**, 3591.

28 M. S. Gordon, J. S. Binkley, J. A. Pople, W. J. Pietro and W. J. Hehre, *J. Am. Chem. Soc.*, 1982, **104**, 2797–2803.

29 J. P. Perdew, K. Burke and M. Ernzerhof, *Phys. Rev. Lett.*, 1996, **77**, 3865.

30 S. Grimme, *J. Comput. Chem.*, 2006, **27**, 1787.

31 C. G. Broyden, *J. Inst. Math. Its Appl.*, 1970, **6**, 222.

32 (*a*) R. F. W. Bader, *Atoms in Molecules - A Quantum Theory*, Oxford University Press, Oxford, 1990; (*b*) R. F. W. Bader, *Chem. Rev.*, 1991, **91**, 893.

33 E. Espinosa, E. Molins and C. Lecomte, *Chem. Phys. Lett.*, 1998, **285**, 170.

34 C. Gatti and S. Casassa, *TOPOND14 User's Manual*, CNR-ISTM Milano, Milano, 2014.

35 (*a*) P. Vinet, J. Ferrante, J. R. Smith and J. H. Rose, *J. Phys. C: Solid State Phys.*, 1986, **19**, L467–L473; (*b*) R. E. Cohen, O. Gulseren and R. J. Hemley, *Am. Mineral.*, 2000, **85**, 338–344.

36 C. G. Ungureanu, R. Cossio and M. Prencipe, *CALPHAD: Comput. Coupling Phase Diagrams Thermochem.*, 2012, **37**, 25–33.

37 (*a*) P. Vinet, J. R. Smith, J. Ferrante and J. H. Rose, *Phys. Rev. B: Condens. Matter Mater. Phys.*, 1987, **35**, 1945–1953; (*b*) Y. Wang, D. J. Weidner and F. Guyot, *J. Geophys. Res.*, 1996, **101**, 661–672.

38 (*a*) Y. Wang, J. J. Wang, H. Zhang, V. R. Manga, S. L. Shang, L. Q. Chen and Z. K. Liu, *J. Phys.: Condens. Matter*, 2010, **22**, 225404; (*b*) S. L. Shang, H. Zhang, Y. Wang and Z. K. Liu, *J. Phys.: Condens. Matter*, 2010, **22**, 375403.

39 (*a*) F. Mouhat and F. Coudert, *Phys. Rev. B: Condens. Matter Mater. Phys.*, 2014, **90**, 224104; (*b*) O. Gomis, H. M. Ortiz, J. A. Sans, F. J. Manjon, D. Santamaria-Perez, P. Rodriguez-Hernandez and A. Munoz, *J. Phys. Chem. Solids*, 2016, **98**, 198–208.

40 (*a*) C. F. Matta and R. J. Boyd, *The Quantum Theory of Atoms in Molecules: From Solid State to DNA and Drug Design*, Wiley-VCH Verlag GmbH & Co. KgaA, Weinheim, 2007; (*b*) S. G. Kozlova, M. R. Ryzhikov and D. G. Samsonenko, *J. Mol. Struct.*, 2017, **1150**, 268.

41 (*a*) D. Cremer and E. Kraka, *Angew. Chem., Int. Ed.*, 1984, **23**, 627; (*b*) E. Espinosa, I. Alkorta, J. Elguero and E. Molins, *J. Chem. Phys.*, 2002, **117**, 5529.

42 (*a*) Yu. V. Nelyubina, M. Yu. Antipin and K. A. Lyssenko, *Russ. Chem. Rev.*, 2010, **79**, 167; (*b*) E. A. Zhurova, A. I. Stash, V. G. Tsirelson, V. V. Zhurov, E. V. Bartashevich, V. A. Potemkin and A. A. Pinkerton, *J. Am. Chem. Soc.*, 2006, **128**, 14728.

43 (*a*) S. J. Grabowski, *Chem. Rev.*, 2011, **111**, 2597; (*b*) D. V. Korabel'nikov and Yu. N. Zhuravlev, *RSC Adv.*, 2019, **9**, 12020–12033.

44 C. Gatti, *Z. Kristallogr.*, 2005, **220**, 399–457.

45 (*a*) J. Joseph and E. D. Jemmis, *J. Am. Chem. Soc.*, 2007, **129**, 4620–4632; (*b*) E. S. Kryachko and T. Zeegers-Huyskens, *J. Phys. Chem. A*, 2001, **105**, 7118–7125.

46 (*a*) D. V. Korabel'nikov, *Phys. Solid State*, 2018, **60**, 571; (*b*) D. V. Korabel'nikov and Yu. N. Zhuravlev, *Phys. Solid State*, 2013, **55**, 1765.

47 (*a*) Yu. N. Zhuravlev and D. V. Korabel'nikov, *J. Struct. Chem.*, 2009, **50**, 1021–1028; (*b*) D. V. Korabel'nikov and Yu. N. Zhuravlev, *Phys. Solid State*, 2017, **59**, 254–261.